Prostate Cancer Detection: Multi-parametric MRI with Diffusion-Weighted Imaging and Dynamic Contrast Enhanced MRI

D. L. Langer[1,2], T. H. van der Kwast[3], A. J. Evans[3], J. Trachtenberg[4], B. C. Wilson[5], and M. A. Haider[1,2]

[1]Joint Department of Medical Imaging, Princess Margaret Hospital, University Health Network and Mount Sinai Hospital, Toronto, Ontario, Canada, [2]Institute of Medical Sciences, University of Toronto, Toronto, Ontario, Canada, [3]Department of Pathology and Laboratory Medicine, Toronto General Hospital, University Health Network, Toronto, Ontario, Canada, [4]Department of Surgical Oncology, Princess Margaret Hospital, University Health Network, Toronto, Ontario, Canada, [5]Medical Biophysics, University of Toronto, Ontario Cancer Institute, Toronto, Ontario, Canada

Introduction

Characterization of tumor location and extent in prostate cancer (PCa) is essential for accurately targeting focal therapies, and may also affect patient management decisions during active surveillance. MRI provides the opportunity to image both anatomy and multiple physiologic properties in the same session. The use of multiple MRI modalities to optimize PCa localization is an active area of study [1-4]; however, interpretation of multi-parametric datasets presents a number of challenges, both in terms of decision making for resolving conflicting results between modalities as well as workload management when review of each image set is required. Generation of a map, developed as a quantitative combination of parameters, would simplify the review process and provide an objective guide for determination of tumor location and boundaries. Our study includes diffusion weighted imaging (DWI), quantitative T2, and dynamic contrast enhanced (DCE) MRI in a radical prostatectomy patient cohort, followed by whole mount pathology. We have explored the optimal combination of parameters for localization of PCa in the peripheral zone (PZ).

Purpose To develop a multi-parametric model suitable for prospective tumor mapping using whole mount pathology during model development.
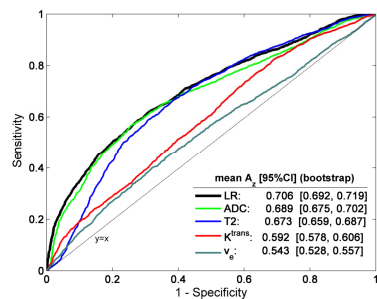
Materials and Methods

Twenty-five men with biopsy-confirmed PCa underwent endorectal MRI on a 1.5T GE Excite HD platform prior to prostatectomy. Ethics board approval and informed consent were obtained. T2-weighted fast-spin echo (FSE) images were acquired, followed by diffusion-weighted imaging (TR/TE = 4000/77ms, 128x256 matrix, 10 NEX, FOV = 14cm, b = 0,600s/mm^2), multi-echo FSE imaging (TR = 2000ms, 10 echo times (9.0-90.0ms), 256x128 matrix, 1 NEX, FOV = 20cm), and dynamic contrast-enhanced (DCE) MRI (TR/TE = 4.3/1.9ms, 256x128 matrix, 0.5 NEX, FOV = 20cm, α = 20°, 10s temporal resolution, 50 phases). All MRI datasets were obtained at identical slice locations with 3mm slice thickness and no intersection gap. ADC and T2 maps were generated, and a Tofts model [5] with assumed arterial input function [6] was used to calculate K^{trans} and v$_e$ maps. The ADC map was re-sampled to match the resolution of all other images. Hematoxylin and eosin stained whole mount sections were prepared to match *in vivo* MRI [7]. PZ tumors >3mm were outlined on all slides by a GU pathologist, and the section with the largest cross-sectional area of tumor used in analyses. All tumors were included; thus, multiple slices were used for patients with multi-focal disease (9 in 25 patients). A region of interest (ROI) in normal PZ was delineated by the pathologist. All tumor and normal ROIs were transferred to MRI. The significance between median tumor and normal values for each parameter in each patient was tested using both unpaired and matched-pair (same-slice tumor and normal ROI) non-parametric tests. Receiver operating characteristic (ROC) curves were generated for each parameter using all ROI voxels. Bootstrapping was used to determine mean areas under the ROC curves (A$_z$s), and to compare performance between parameters. Feature vectors (FVs) for logistic regression (LR) modeling were generated, corresponding to the set of parameter values at each spatial location within each ROI (*i.e.*, a subset of {ADC(*i,j*), T2(*i,j*), K^{trans}(*i,j*), v$_e$(*i,j*)}). The model was optimized by adding parameters step-wise based on decreasing A$_z$, testing each parameter addition for significance and accounting for correlated data within patients. The final model was compared against each parameter. Bonferroni-adjusted α's were used for multiple comparison significance tests.

Results and Discussion

Thirty-eight tumors from the twenty-five patients were reviewed. Median ADC and T2 values in PCa (1.275 x10^{-3}mm^2/s and 88.7ms, respectively) were significantly lower than in benign PZ (1.467 x10^{-3}mm^2/s and 111.6ms, respectively) both overall (P<0.005), and for matched-pair tests (P<0.001).   There were no overall differences between tumor and normal values for K^{trans} nor v$_e$ (PCa and normal: 0.298 and 0.253 min^{-1} for K^{trans} (P=0.168), 0.283 and 0.290 for v$_e$ (P=0.670)); however, in matched-pair tests, median K^{trans} values in PCa were significantly higher than normal PZ (P=0.013), and v$_e$ values showed a trend towards being significantly lower (P=0.069). 6460 voxels were extracted from all ROIs (4152 PCa, 2308 benign). ADC had the highest ROC performance (mean A$_{z,ADC}$: 0.689), and was significantly greater than A$_{z,Ktrans}$ (mean: 0.592, P<0.002) or A$_{z,ve}$ (mean: 0.543, P<0.002), but not A$_{z,T2}$ (mean: 0.673, P=0.026). Additions of ADC, T2, and K^{trans} to the LR-model were significant, with the probability of a voxel being malignant determined as Pr=e^z/(1+e^z), where z=3.176-1378ADC-0.0089T2+0.715K^{trans}. A$_{z,LR}$ (mean: 0.706) was significantly higher than A$_z$ for T2, K^{trans}, and v$_e$ (P<0.002), and was higher than A$_{z,ADC}$, however not significantly (P=0.09). ROC curves for all parameters and LR-model are in Figure 1. Our A$_z$ values are on the low range of those reported (0.66-0.91) [1-4], but reflect the variability in voxel data versus overall detection of a ROI. Our approach ensures the training set reflects input data for mapping, especially in the case where median values in ROIs occur in different spatial locations for each parameter [1]. Although there are many multi-parametric methods, LR provides an attractive option; after training, the model can be applied prospectively to new datasets, yielding maps of continuous malignant-probability. Input maps and resulting LR map are shown in Figure 2. MRI values for central gland (CG) tissue differ from PZ, necessitating separate training sets to extend this work to CG. The limited number of CG tumors in our patient cohort (4 in 25 patients) precluded this analysis. ADC was the best performing single parameter, and although the LR model had a higher A$_z$, the difference was not significant. However, the addition of T2 and K^{trans} was significant in the model, and may lead to a method to detect PCa with ADC values comparable to normal PZ.
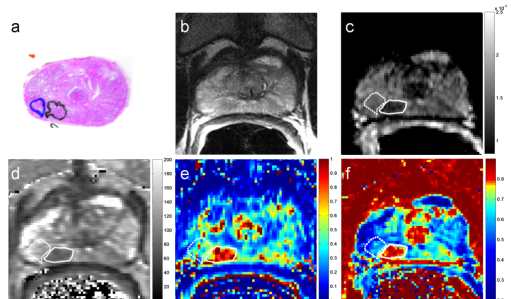
Conclusion

We have developed a multi-parametric model incorporating ADC, T2 and K^{trans} to create a single quantitative map of tumor probability, which may improve localization of cancer in the peripheral zone of the prostate.

Figure 2. Whole mount section (**a**), T2-weighted MRI (**b**), input parameter maps ADC (**c**), T2 (**d**), and K^{trans} (**e**), and LR map using final model (**f**). (map valid for PZ tissue) tumor: black/solid line, normal: blue/dotted line) The lesion is clearly visible in (**f**), with much of the noise from the input datasets removed. The tumor/normal regions identified were added to the overall training dataset.

Figure 1 legend (in plot):
mean A$_z$ [95%CI] (bootstrap)
LR: 0.706 [0.692, 0.719]
ADC: 0.689 [0.675, 0.702]
T2: 0.673 [0.659, 0.687]
K^{trans}: 0.592 [0.578, 0.606]
v$_e$: 0.543 [0.528, 0.557]

Figure 1. ROC curves for all parameters and LR-model. ADC was the top single-parameter; A$_{z,ADC}$ was significantly higher than A$_z$ for K^{trans}, and v$_e$, and greater than T2 (not significant). LR was significantly better than T2, K^{trans}, and v$_e$, and greater than ADC (not significant).

References [1] Kozlowski *et al*, JMRI 2006; 24:108-113. [2] Futterer *et al*, Radiol 2006; 241:449-458. [3] Reinsberg *et al*, AJR 2007; 188:91-98. [4] Mazaheri *et al*, Radiol 2008; 246:480-488. [5] Tofts. JMRI 1997;7:91-101. [6] Fritz-Hansen *et al*, MRM 1996; 36:225-231. [7] Langer *et al*, Proc. Intl. Soc. Mag. Reson. Med. Berlin 2007, 747.